Available online at www.sciencedirect.com

ScienceDirect

J Materiomics 1 (2015) 348–356

www.ceramsoc.com/en/

www.journals.elsevier.com/journal-of-materiomics/

Electrical transport properties of nano crystalline Li–Ni ferrites

G. Aravind [a], M. Raghasudha [b,*], D. Ravinder [a]

[a] Department of Physics, Osmania University, Hyderabad, 500 007, Telangana, India
[b] Department of Chemistry, Jayaprakash Narayan College of Engineering, Mahabubnagar, 509001, Telangana, India

Received 18 April 2015; revised 18 September 2015; accepted 19 September 2015
Available online 14 October 2015

Abstract

Nickel substituted lithium nano ferrites with the chemical composition $Li_{0.5-0.5x}Ni_xFe_{2.5-0.5x}O_4$ ($0.0 \leq x \leq 1.0$) were prepared by Citrate-gel method. The single phase cubic spinel structure of the ferrites was confirmed by X-ray diffraction analysis. Surface morphology and particle size of the samples was studied using Transmission Electron Microscopy (TEM). The TEM micrographs reveal that the particle size of the samples was in the nanometric range confirming the nano crystalline nature. The FTIR spectra shows the two significant absorption bands in the wave number range of 400–600 cm^{-1} arising due to the inter-atomic vibrations in the tetrahedral and octahedral coordination compounds. The dielectric parameters like dielectric constant (ε'), dielectric loss tangent ($\tan\delta$) and AC conductivity (σ_{ac}) of the samples were measured using LCR meter at room temperature in the frequency range 20 Hz–2 MHz ε', $\tan\delta$ and σ_{ac} of the samples show a normal dielectric behavior of ferrites with frequency which indicates the fact that the dielectric dispersion is due to the hopping of electrons between the Fe^{2+} and Fe^{3+} ions. Thermo Electric Power (TEP) studies of Li–Ni ferrites were measured using differential method in the temperature range of 473–873 K. Seebeck coefficient (S) of the prepared ferrites was increased with increasing temperature.
© 2015 The Chinese Ceramic Society. Production and hosting by Elsevier B.V. This is an open access article under the CC BY-NC-ND license (http://creativecommons.org/licenses/by-nc-nd/4.0/).

Keywords: Ferrites; Citrate gel method; X-ray diffraction; Dielectric behavior; Thermo electric power

1. Introduction

Ferro-spinels have interesting structural, electrical and magnetic properties. They are widely used in many important applications such as microwave devices like circulators, phase shifters, memory cores, magnetic recording media, transformers, choke coils, high frequency instruments, data storage, noise filters and recording heads, owing to their high magnetic permeability and low magnetic loss [1]. The usefulness of a ferrite material for microwave devices is influenced by physical and chemical properties which in turn depend on the method of preparation [2]. For obtaining the required properties, selection of the ferrite composition and nature of substituent ion is most important besides sintering temperature and time. The valence state of doping ions in the selected ferrite composition influences the structural, electrical and magnetic properties of ferrite material.

Ferrite materials are low mobility semiconducting iron oxides. Unlike most materials, they possess high permeability and moderate permittivity at different frequencies. Due to their small eddy current losses, they possess wide range of electronic applications in terms of energy production, transmission and telecommunication applications. At present, 'nano ferrites' has been the subject of many scientists all over the world because of novel properties exhibited by nano-particles. The properties of bulk material vary drastically when their size approaches the nano-scale [3]. In ferrites, grain size reduction and grain boundary modifications results in high frequency properties such as resistivity and quality factors. Smaller grain size will provide large number of grain boundaries as barriers for the electron hopping between the different ions so as to increase the resistivity and decrease the eddy current losses in ferrites [4].

* Corresponding author. +919550083100 (mobile).
E-mail address: raghasudha_m@yahoo.co.in (M. Raghasudha).
Peer review under responsibility of The Chinese Ceramic Society.

http://dx.doi.org/10.1016/j.jmat.2015.09.003
2352-8478/© 2015 The Chinese Ceramic Society. Production and hosting by Elsevier B.V. This is an open access article under the CC BY-NC-ND license (http://creativecommons.org/licenses/by-nc-nd/4.0/).

Lithium ferrites and substituted Lithium ferrites have become most attractive materials for microwave applications especially as a replacement for garnets. Mixed lithium ferrites have low cost, square hysteresis loop, high Curie temperature that make them promising materials for microwave applications [5–7].

Nano-crystalline ferrite materials can be synthesized by various preparation techniques including glass-ceramic method [8], hydrothermal method [9], sol–gel method [10], co-precipitation method [11], and citrate-gel method [12]. Many scientists have studied the frequency dependence on the dielectric properties of Li–Co [13], Li–Mg [14], Li–Ge [15]. Among the various preparation methods citrate-gel auto-combustion method has attracted the attention of solid state chemist, physicist and material scientist etc. due to the fact that the product with high purity, good homogeneity and low particle size can be obtained. This is because the mixing of constituent cations takes place on atomic scale in the precursor itself, thereby lowering the sintering temperature during the formation of required ferrites. Moreover, novel properties for the product were observed in this method of preparation [16]. Some authors have synthesized nickel substituted lithium ferrites by ceramic method with high sintering temperature [17]. However, there is no detail report on Ni substituted Lithium nano ferrites prepared by citrate-gel auto combustion method with low sintering temperature.

In the present work, the authors report the structural properties of Li–Ni nano crystalline ferrites with XRD, TEM and FTIR analysis with the detailed investigation of the composition. Frequency dependence of the dielectric properties and thermo electric power studies of the samples with the results were discussed.

2. Experimental

Ni substituted Lithium ferrites with compositional formula $Li_{0.5-0.5x}Ni_xFe_{2.5-0.5x}O_4$ (where x = 0.0 to 1.0) with a step increment of 0.2 have been prepared by low temperature citrate gel auto combustion method with the following raw materials as starting chemicals:

(i) Ferric nitrate ($Fe(NO_3)_2 9H_2O$)
(ii) Nickel nitrate ($Ni(NO_3)_2 6H_2O$)
(iii) Lithium nitrate ($LiNO_3$)
(iv) Citric acid ($C_6H_8O_7 \cdot H_2O$) and Ammonia solution (NH_3).

The detailed procedure for the preparation of ferrites by citrate-gel auto-combustion method was explained in our earlier publication [18]. The synthesized powders were sintered at 500 °C for 4 h in air at a slow heating rate of 5 °C/min and then furnace cooled. X-ray diffraction analysis of the prepared ferrite powders were performed by using Philips X-ray diffractometer with Cu K_α radiation of wavelength 1.5405 A°. The average crystallite size of the ferrites was determined from the measured width of their diffraction pattern using the Debye Scherer's formula

$$D = \frac{0.91\lambda}{\beta \cos\theta} \quad (1)$$

Where λ-the wavelength of the x-ray used for diffraction,

β – full width half maximum (FWHM) in radians.
θ – diffraction angle.

The lattice constant 'a' was calculated using the following relation

$$a = d\left(h^2 + k^2 + l^2\right)^{1/2} \quad (2)$$

where d-inter planar distance, hkl-miller indices

Hopping length for tetrahedral site (d_A) and octahedral site (d_B) can be calculated using

$$d_A = 0.25a\sqrt{3}A^0 \quad \& \quad d_B = 0.25a\sqrt{2}A^0 \quad (3)$$

The morphology of prepared ferrites was investigated using Transmission Electron Microscopy with a JEOL 2000 electron microscope operating at 200 kV.

The FTIR spectra of the ferrite samples as pellets in KBr were recorded by SHIMADZU FTIR spectrophotometer in the frequency range of 400–600 cm^{-1}

For the thermo electric power measurements, the synthesized powders were made in the form of circular pellets (diameter – 13 mm and thickness – 2 mm) using 2% polyvinyl alcohol (PVA) as binder under a pressure of 5 tons for 1–2 min. These pellets were finally sintered at 500 °C for 4 h and then slowly cooled to room temperature. Pellets were then coated on either side with a thin layer of silver paste to have good electrical contact.

Agilent E4980A Precision LCR meter was used for the dielectric measurements of the prepared pellets by using bellow formulae [19,20].

$$\text{Real part of dielectric constant } (\varepsilon') = C\,d/A\,\varepsilon_0 \quad (4)$$

$$\text{Imaginary part of dielectric constant } \varepsilon'' = (\varepsilon')\tan\delta \quad (5)$$

$$\text{AC conductivity} \quad \sigma_{ac} = 2\pi f\,\varepsilon_o(\varepsilon')\tan\delta \quad (6)$$

Where C – capacitance of the pellet in faraday

$\tan\delta$ – dielectric loss tangent.
ε_0 – permittivity of free space = 8.85×10^{-12} F/m
f – frequency

Thermo electric power measurement studies on the prepared pellets were carried out by differential method from 320 K to well beyond Curie temperature. The pellet was kept between the hot and cold junctions of the method. The temperature difference between two ends of the sample was kept at 10 K throughout the measured temperature range. The thermo emf was produced across the sample as the charge carriers (electrons or holes) diffused from the hot junction to the cold junction due to the temperature gradient ΔT in degree Kelvin maintained across the sample.

The thermo electric power or Seebeck coefficient (S or α) was calculated using the following relation [21].

$$S = \frac{\Delta E}{\Delta T}(\mu V/K) \quad (7)$$

where ΔE is the thermo electro motive force produced across the two ends of the sample which is measured by using a digital micro voltmeter and the ΔT is the temperature difference between the two surfaces of the pellet which is measured by two chromel-alumel thermocouples that were kept very close to the sample. For achieving good thermal stability, thermo emf values were measured while cooling.

The carrier concentration values of the prepared samples were calculated using the following relation

$$n = Ne^{(-Se/K)} \quad (8)$$

where N – concentration of electronic levels involved in the conduction process

S – Seebeck coefficient
e – electron charge, K – Boltzmann constant.

Ferrites are low mobility semiconductors having exceedingly narrow bands or localized levels, so value of N can be taken as 10^{22}/mL [22].

3. Results and discussions

3.1. X-ray diffraction analysis

The X-ray diffraction pattern of the prepared Ni substituted Lithium nano ferrites were shown in Fig. 1.

The diffraction patterns confirmed the well defined homogeneous single phase cubic spinel structure of the samples without any impurity peak belonging to the space group $P4_332$ (confirmed by JCPDS No.88-0671).

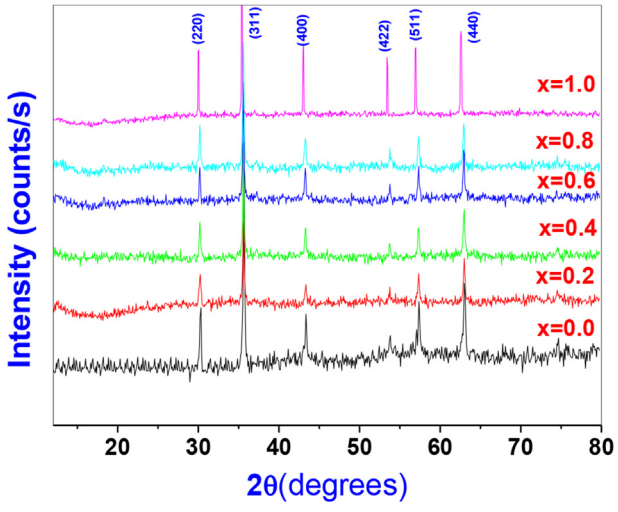

Fig. 1. XRD pattern of the nano crystalline $Li_{0.5-0.5x}Ni_xFe_{2.5-0.5x}O_4$ ferrites.

Table 1
Lattice parameter, Crystallite size and hoping length for $Li_{0.5-0.5x}Ni_xFe_{2.5-0.5x}O_4$ ferrites.

Ferrite composition	Lattice parameter (Å)	Crystallite size (nm)	Hopping length	
			A-site (d_A)	B-site (d_A)
$Li_{0.5}Fe_{2.5}O_4$	8.356	41.90	3.618	2.953
$Li_{0.4}Ni_{0.2}Fe_{2.4}O_4$	8.356	39.54	3.618	2.954
$Li_{0.3}Ni_{0.4}Fe_{2.3}O_4$	8.358	45.35	3.619	2.954
$Li_{0.2}Ni_{0.6}Fe_{2.2}O_4$	8.361	49.90	3.620	2.955
$Li_{0.1}Ni_{0.8}Fe_{2.1}O_4$	8.368	41.30	3.623	2.958
$NiFe_2O_4$	8.374	43.01	3.626	2.960

All the diffraction peaks were indexed as (220), (311), (400), (422), (511) and (440) that confirm the pure spinel phase of the prepared ferrites. Crystallite size of the prepared samples measured from the X-ray analysis by Debye Scherer's formula was in the range of 39–49 nm as shown in Table 1. From the table it is clear that with increase in Ni composition in the Li–Ni ferrites, Lattice parameter of the prepared samples was increased. This was expected because six fold co-ordinated ionic radius of the Ni^{2+} (0.78 Å) was greater than the six fold co-ordinated ionic radii of the Li^+ (0.76 Å) and Fe^{3+}(0.67 Å) ions.

Hopping length of A-site and B-site was observed to be increased with increase in the Ni composition. This is because, hopping length of the sites were directly proportional to the lattice parameters of the samples. The variation of lattice parameter (Å) and hopping length of A-site with Ni compositions were shown in Fig. 2a and b respectively.

3.2. FTIR spectral analysis

The FTIR spectra of nickel substituted lithium ferrites measured in the frequency range of 400 cm^{-1}–600 cm^{-1} were shown in Fig. 3. From the figures, it is noticeable that the two main absorption bands appeared common in almost all spinel ferrites of the ferrite system under investigation. These absorption bands are observed around 600 cm^{-1} and 400 cm^{-1} respectively and are summarized in Table 2. These bands correspond to the stretching vibrations of tetrahedral (A) (ν_1) and octahedral (B) (ν_2) sites respectively which represent the characteristic feature of single phased spinel ferrites [23].

The observed larger ν_1 values of the prepared ferrites compared to the ν_2 values indicates the normal mode of vibration in these ferrites. This is because of shorter bond length of A-site compared to that of B site. In Li–Ni ferrites, an absorption band ν_3 was observed for $x < 0.6$, the values of which are summarized in Table 2. According to Tarte [24], the recorded band ν_3 indicates the presence of Li–O complexes on the octahedral sites. The intensity of this band goes on decreasing with increase in the nickel substitution in the system. This is because, Li^+ content decrease with increase in x, so it persists only up to $x = 0.6$ and then it completely disappears [25]. The shift occurred in the absorption band ν_1, ν_2 for each A and B sites are due to the perturbation occurring in the Fe–O band by introducing Ni composition in the Li–Ni mixed ferrites.

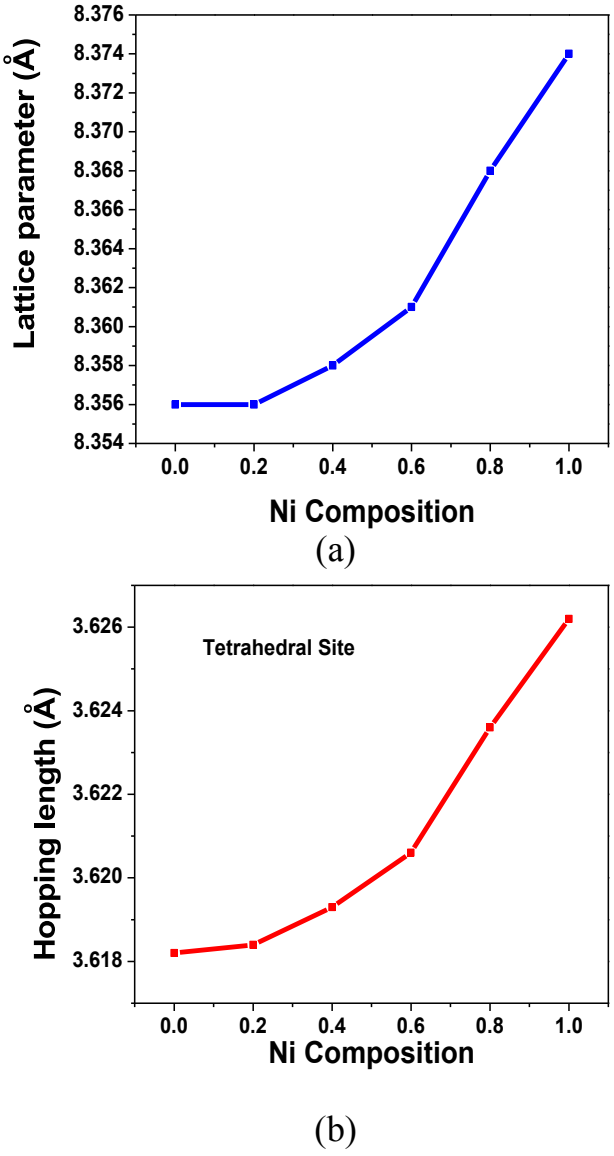

Fig. 2. a. Variation of lattice constant of $Li_{0.5-0.5x}Ni_xFe_{2.5-0.5x}O_4$ ferrites with Ni composition. b. Variation of hopping length of A site (d_A) of $Li_{0.5-0.5x}Ni_xFe_{2.5-0.5x}O_4$ ferrites with Ni composition.

From Table 2, one can observe that the tetrahedral vibrational band (ν_1) appeared in the range of 549–552 cm^{-1}, octahedral vibrational band (ν_2) in the range of 414–430 cm^{-1} and Li–O band (ν_3) in the range of 444–458 cm^{-1}.

3.3. TEM analysis of Li–Ni ferrites

The particle size, shape and size distribution are important morphological characteristics for a nano scaled material [26]. Transmission electron microscopy (TEM) provides a direct information about these characteristics. TEM micrographs of the prepared Li–Ni ferrite samples annealed at 500 °C for 4 h are shown in Fig. 4 which are nearly spherical in shape. The average particle size observed from the TEM micrographs suggests the formation of single crystals [27].

3.4. Dielectric properties

The dielectric properties of the ferrites depends on the several factors including method of preparation, sintering time, sintering temperature, particle size, type and amount of substitution, etc. Dielectric parameters at room temperature in the frequency range of 20 Hz–2 MHz were calculated using the relations 4, 5, 6. The frequency dependence of real part of dielectric constant (ε') and imaginary part of dielectric constant (ε'') at room temperature were shown in Fig. 5 (a) and (b). From the figures, it is clear that the value of ε' and ε'' decreases continuously with increasing frequency. After certain frequency, the dielectric parameters do not change with frequency i.e. become independent of frequency. This fact shows a normal behavior of ferromagnetic materials.

The variation of dielectric constant with frequency may be explained on the basis of space-charge polarization phenomenon [28]. According to this, dielectric material has well conducting grains separated by highly resistive grain boundaries. On the application of electric field, space charge accumulates at the grain boundaries and voltage drops mainly at grain boundaries [29]. Koops proposed that grain boundary affect is more at low frequencies [29]. As the frequency increased beyond a certain limit the electron exchange between Fe^{2+} and Fe^{3+} ions does not follow the variations in applied field, so the value of dielectric constant becomes constant.

The variation in the dielectric parameters with frequency in ferrites was through a mechanism similar to the conduction process [30]. The electron exchange between Fe^{2+} and Fe^{3+} ions results in local displacement of electrons in the direction of applied field that determines polarization. The Polarization decreases with increasing frequency, and then reaches a constant value. It is due the fact that beyond a certain frequency of external field, the electron exchange $Fe^{2+} \leftrightarrow Fe^{3+}$ cannot follow the alternating field. The high value of dielectric constant at lower frequency is due to the predominance of the species like Fe^{2+} ions, oxygen vacancies, grain boundary defects, etc [31] while the decrease in dielectric constant with frequency is natural, i.e. any species contributing to the polarizability is found to show the applied field lagging behind at higher frequencies [32]. Hence, the electron conduction mechanism can be explained by electron hopping between the same element having the different ionic states (Fe^{3+}/Fe^{2+} and Ni^{2+}/Ni^{+}) [33].

Variation of loss tangent of the material with frequency was shown in Fig. 6. From the figure, it is observed that tan δ decrease with increase in frequency and the values were very small at high frequencies. Hence, these materials are desirable for high frequency microwave device applications. The variation of dielectric constant of Li–Ni nano ferrites with Ni composition was shown in Fig. 7. From the figure, it is observed that room temperature dielectric constant decreased with increase in Ni concentration after an initial rise of Ni concentration from 0.0 to 0.2. It is seen that as Ni content is increased there is a decrease in the Fe^{3+} ions at the B-sites thereby decreasing the hopping of electrons, that results in

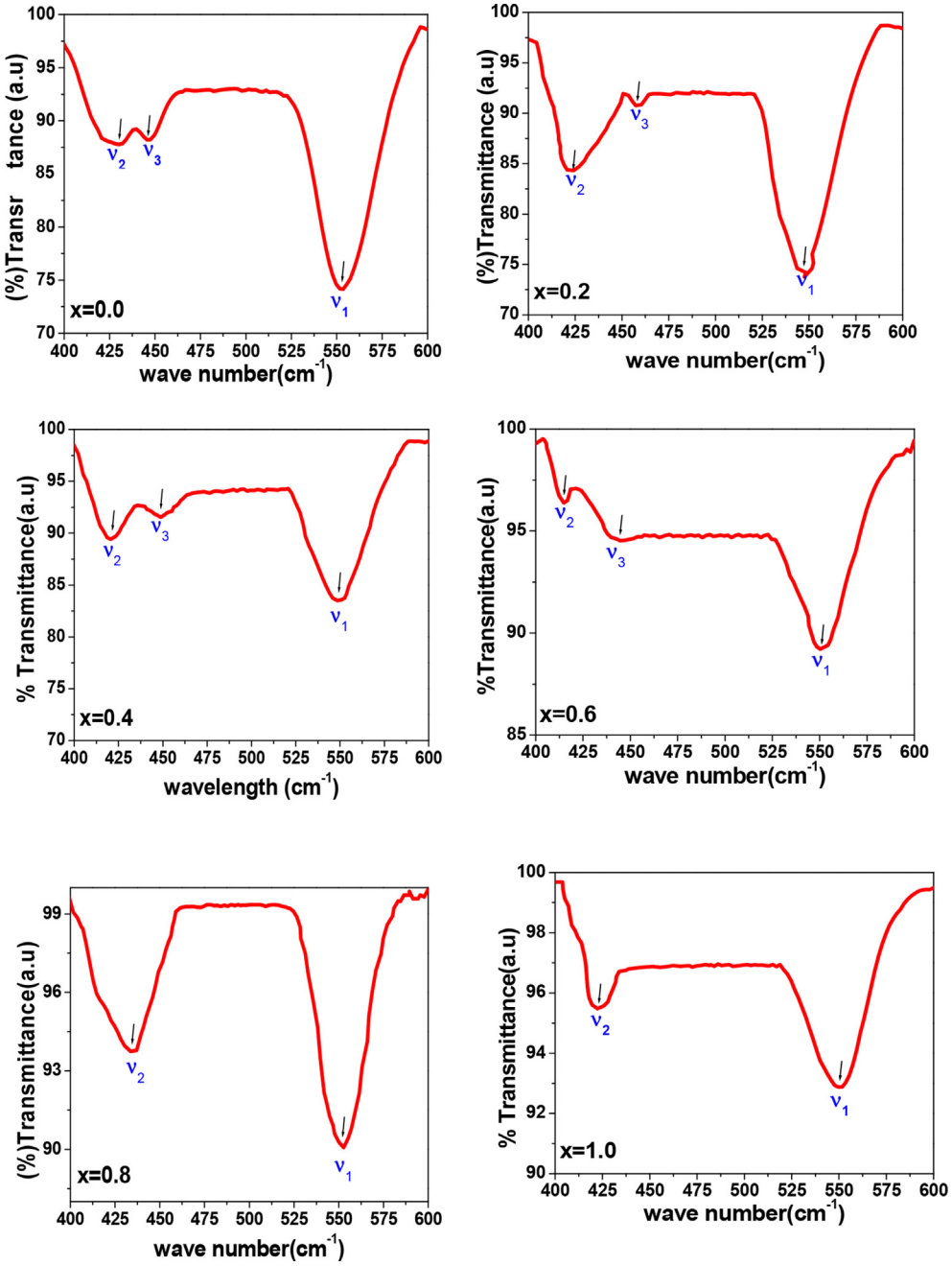

Fig. 3. FTIR absorption spectra of the $Li_{0.5-0.5x}Ni_xFe_{2.5-0.5x}O_4$ ferrite samples ($0.0 \leq x \leq 1.0$).

decrease in piling up of electrons at the grain boundary. Therefore, the dielectric constant decreases. The same anomalous behavior was also observed by some researchers [34].

Table 2
Band positions of the Li–Ni ferrites estimated from the FTIR spectroscopy.

Composition	ν_1 (cm^{-1})	ν_2 (cm^{-1})	ν_3 (cm^{-1})
$Li_{0.5}Fe_{2.5}O_4$	552	430	446
$Li_{0.4}Ni_{0.2}Fe_{2.4}O_4$	549	423	458
$Li_{0.3}Ni_{0.4}Fe_{2.3}O_4$	550	420	449
$Li_{0.2}Ni_{0.6}Fe_{2.2}O_4$	552	414	444
$Li_{0.1}Ni_{0.8}Fe_{2.1}O_4$	553	433	–
$NiFe_2O_4$	550	422	–

Frequency dependence of AC conductivity of the prepared ferrites was shown in Fig. 8. From the figure, it is observed that the AC conductivity of the prepared samples shows dispersion with respect to frequency. At lower frequencies, AC conductivity is almost constant. But, after certain frequency it increases rapidly. This behavior can be explained by Koop's theory [35], which supported that the ferrite material act as a bilayer condenser. According to Koop's bilayer model in ferrite, first layer is a conducting layer consisting conducting ferrite grains which is separated by a second layer of poorly conducting intermediate grain boundaries. Koops proposed that grain boundary effect dominates at lower frequencies resulting in low conductivity. With increase in frequency the

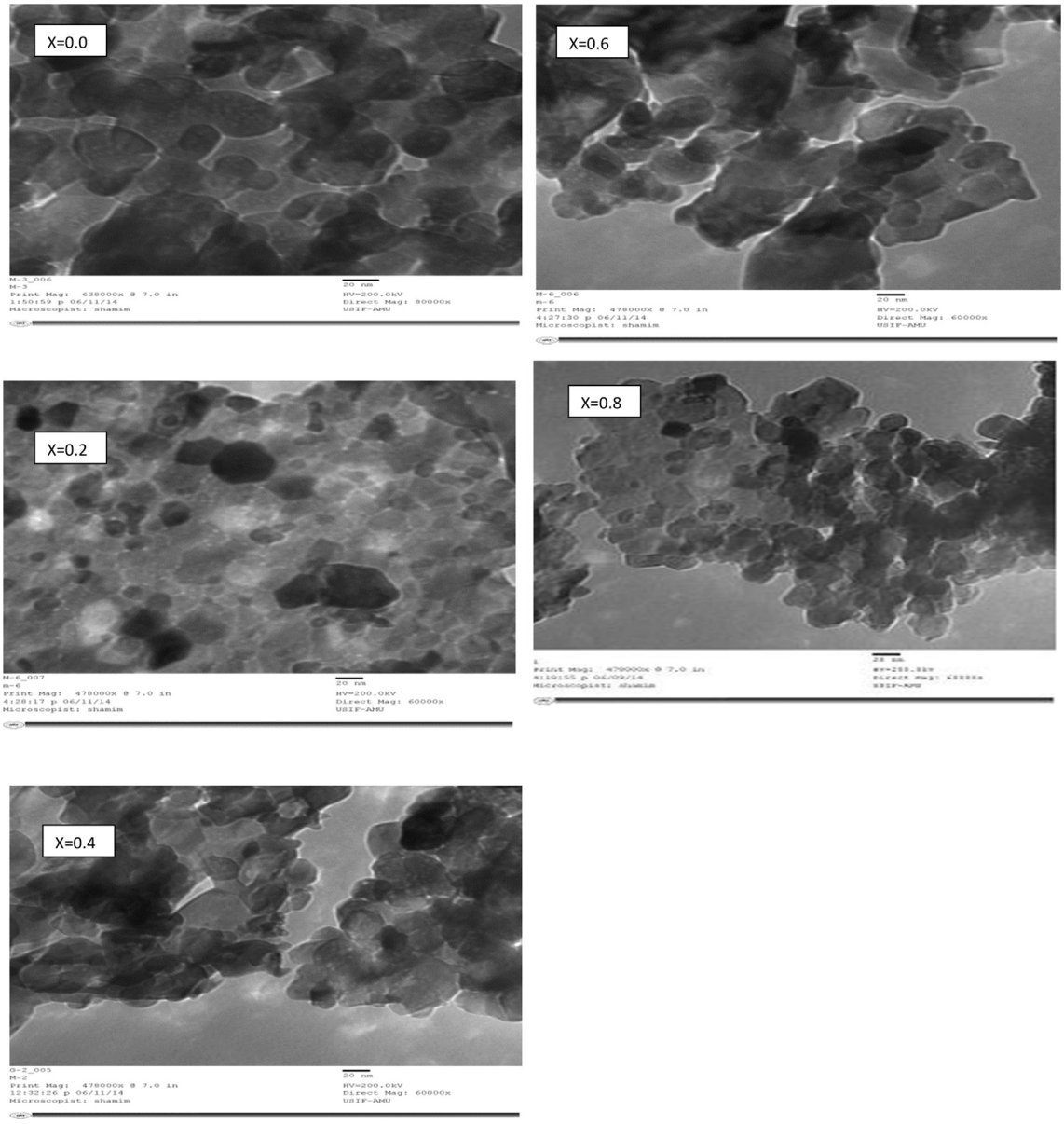

Fig. 4. TEM micrographs of nano crystalline $Li_{0.5-0.5x}Ni_xFe_{2.5-0.5x}O_4$ ferrites (x = 0.0 to 0.8).

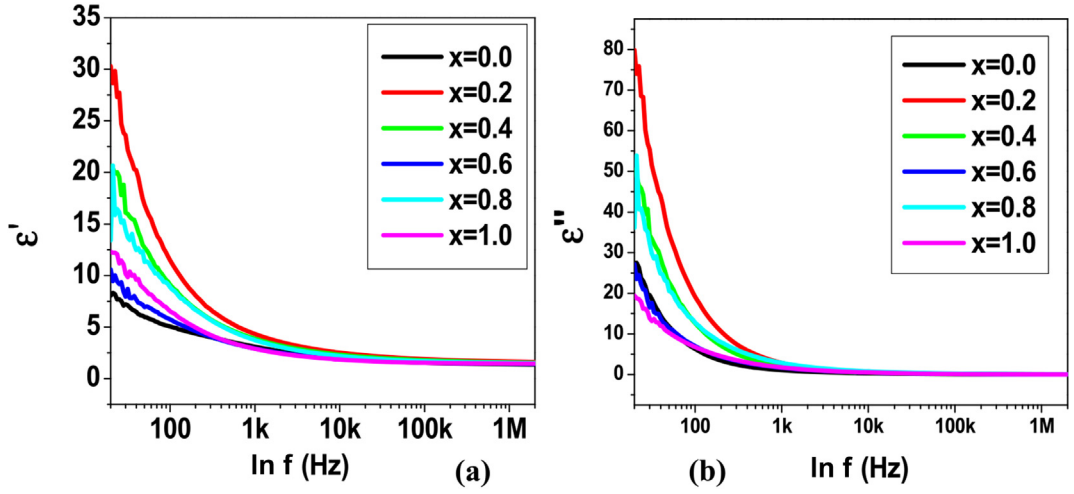

Fig. 5. Variation of (a) real part of dielectric constant (ε') and. (b) imaginary part of dielectric constant (ε'') with frequency.

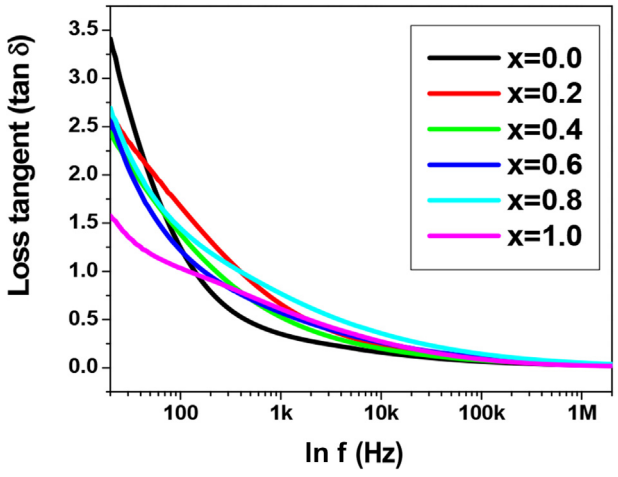

Fig. 6. Variation of Loss Tangent with frequency of $Li_{0.5-0.5x}Ni_xFe_{2.5-0.5x}O_4$ ferrites.

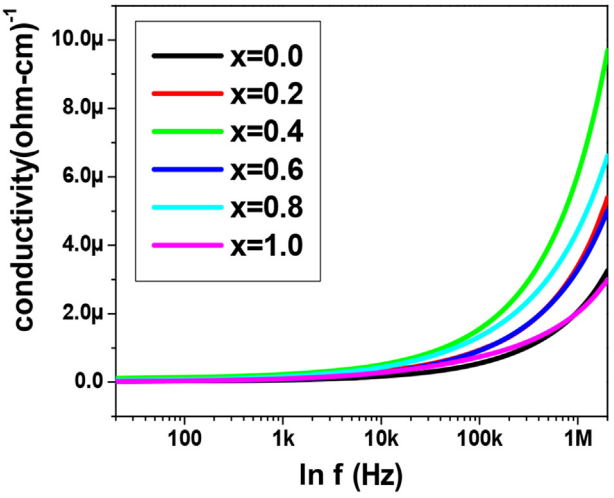

Fig. 8. Variation of AC conductivity with frequency of $Li_{0.5-0.5x}Ni_{x}Fe_{2.5-0.5x}O_4$ ferrites.

conductive grains becomes more dominating resulting in promoting the hopping between Fe^{2+} and Fe^{3+} ions and hence the conductivity increases.

3.5. Thermo electric power studies

The Variation of Seebeck coefficient (S) with temperature of the prepared Li–Ni ferrites was shown in Fig. 9. From the figure, it was observed that all the samples show similar thermal variation with S and the value of S increases with increase in the temperature.

At low temperature, positive value of S shows p-type semi conducting nature of the prepared ferrites. By increasing the temperature, the sample has changed to n-type semiconductor behavior. The probable conduction mechanisms in the spinel ferrite system under investigation are

$$Fe^{2+} \leftrightarrow Fe^{3+} + e^{-} (n-\text{type or electron exchange mechanism})$$

$$Ni^{2+} \leftrightarrow Ni^{1+} + e^{+} (p-\text{type or hole exchange mechanism})$$

The preponderance of one mechanism over the other depends upon the concentration of substituted cation and temperature. If the hole exchange mechanism dominates over the electron exchange mechanism, the ferrite composition might conduct as p-type semiconductor or vice versa. On increasing the temperature the n-type of conduction mechanism becomes more probable which generates electrons and the material behaves as n-type semiconductor at higher temperature. Hence the material was behaving as p-type semiconductor at low temperature region and changes to n-type at high temperature region.

Li–Ni ferrite samples show an increasing trend in Seebeck coefficient with temperature which indicates that more n-type charge carriers (electrons) are released with an increase in temperature. At a particular temperature an abrupt change was occurred which is called Curie temperature. From the figure, one can say that

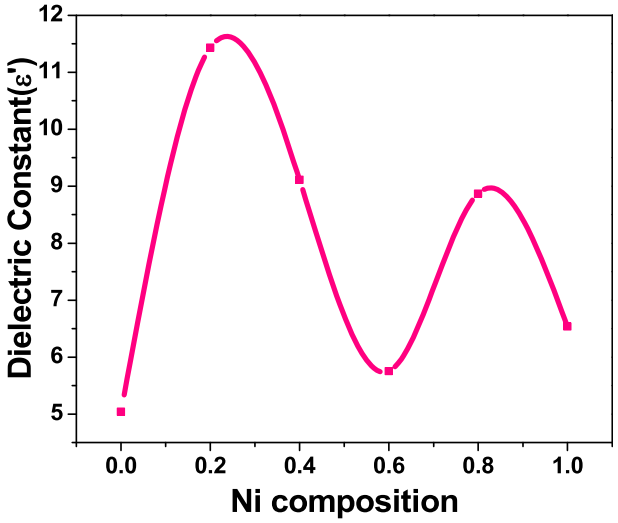

Fig. 7. Variation of dielectric constant (ε') with Ni composition.

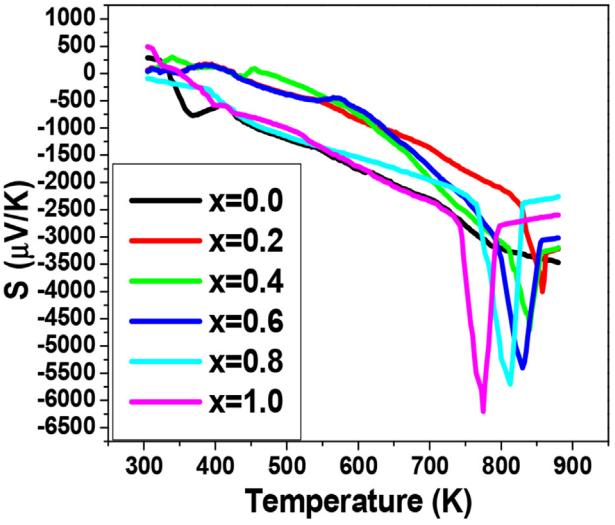

Fig. 9. Variation of Seebeck coefficient with temperature of $Li_{0.5-0.5x}Ni_xFe_{2.5-0.5x}O_4$ ferrites.

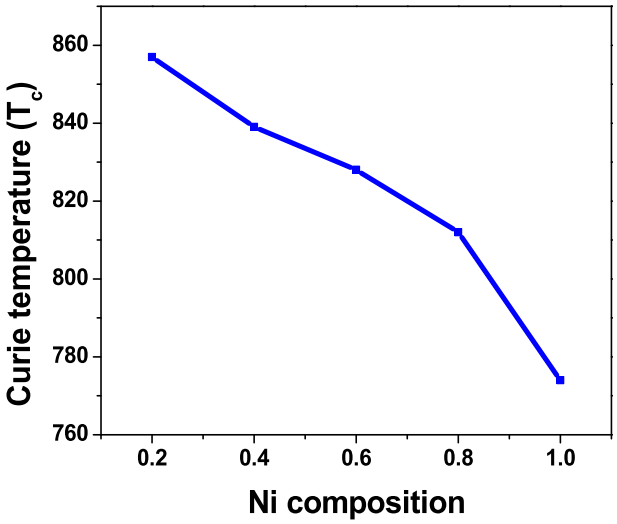

Fig. 10. Variation of Curie temperature with Ni composition.

the Curie temperature of the prepared samples decreased with increase in the Ni concentration in the Li–Ni ferrite system (see Table 3).

Variation of Curie temperature with Ni composition of the prepared ferrites was shown in Fig. 10. The decrease in Curie temperature by increasing the Ni doping can be understood on the basis of the number of magnetic ions present in the two stable sub lattices and mutual interaction. An increase in the Ni^{2+} at the octahedral site has replaced the Fe^{3+} at this site. This leads to the decrease in the AB interaction of the type $Fe_A^{3+} - O^{2-} - Fe_B^{3+}$. Curie temperature depends on overall strength of AB exchange interaction, so the weakening of the $Fe_A^{3+} - O^{2-} - Fe_B^{3+}$ interaction results in a decrease in Curie temperature of prepared Li–Ni ferrites [36].

Carrier concentration of the prepared samples was calculated at 500 K. It can be seen from the Table 3 that among all the mixed Li–Ni spinel ferrites, the composition$Li_{0.1}$ $Ni_{0.8}Fe_{2.1}O_4$was having the highest values of carrier concentration.

4. Conclusions

Ni^{2+} ions when substituted in the basic lithium ferrite affect its structural and dielectric properties. The crystallite size of the prepared samples was in the range of 39–49 nm which reveals the nano crystalline structure. An increase in the Ni concentration increase the lattice parameter and hopping length of A-site and B-site. The dielectric constant and dielectric loss tangent were observed to decrease with the increase in frequency, which was the common nature of any semiconducting ferrites. The AC conductivity of the prepared samples was observed to increase with increasing the frequency. Seebeck coefficient of the prepared Li–Ni ferrite samples were increased with increase in temperature. Curie temperature of the samples was observed to be decreased with increasing Ni concentration in the Li–Ni nano crystalline ferrites.

Table 3
Seebeck coefficient, Carrier concentration, Curie temperature of Li–Ni ferrites.

Composition	Seebeck coefficient (μV/K)	Carrier concentration (n)	Curie temp (K)
$Li_{0.5}Fe_{2.5}O_4$		3.26×10^{22}	>900
$Li_{0.4}Ni_{0.2}Fe_{2.4}O_4$	3974	1.59×10^{22}	857
$Li_{0.3}Ni_{0.4}Fe_{2.3}O_4$	4648	1.15×10^{22}	839
$Li_{0.2}Ni_{0.6}Fe_{2.2}O_4$	5350	1.61×10^{22}	828
$Li_{0.1}Ni_{0.8}Fe_{2.1}O_4$	5670	3.64×10^{22}	812
$NiFe_2O_4$	6100	3.04×10^{22}	774

Acknowledgment

The authors are very grateful to Prof. R.Sayanna, Head, Department of Physics, University College of Science, Osmania University, Hyderabad. The authors are very thankful to UGC, New Delhi, for their financial assistance through Major research Project (M.R.P).

References

[1] Goodenough JB. In: Cotton FA, editor. Magnetism and the chemical bond, interscience monographs on chemistry, inorganic chemistry section, vol. I. New York: Interscience-Wiley; 1963.
[2] Liu C, Lan Z, Jiang X, Yu Z, Sun K, Li L, et al. Effects of sintering temperature and Bi_20_3 content on microstructure and magnetic properties of Li–Zn ferrites. J Magn Magn Mater 2008;320:1335.
[3] Kumar AM, Verma MC, Dube CL, Rao KH, Kashyap SC. Development of Ni–Zn nano ferrite core material with improved saturation magnetization and DC resistivity. J Magn Magn Mater 2008;320:1995.
[4] Yang YJ, Sheu CI, Cheng SY, Chang HY. Si–Ca species modification and microwave sintering for Ni–Zn ferrites. J Magn Magn Mater 2004;284:220.
[5] Jadhav SA. Magnetic properties of Zn-substituted Li–Cu ferrites. J Magn Magn Mater 2001;224:167.
[6] Shaikh AM, Kanamadi CM, Chougule BK. Electrical resistivity and thermo electric power studies of Zn substituted Li–Mg ferrites. Mater Chem Phys 2005;93:548.
[7] Jadhav SA. Structural and magnetic properties of Zn substituted Li–Cu ferrites. Mater Chem Phys 2000;65:120.
[8] El-Sayed Ahmed M, Hamzawy Esmat MA. Structure and magnetic properties of Nickel–Zinc ferrite nanoparticles prepared by glass crystallization method. Monatsh für Chemie/Chemical Mon 2006;137:1119. http://dx.doi.org/10.1007/s00706-006-0521-1.
[9] Hu Chaoquan, Gao Zhenghong, Yang Xiaorui. One-pot low temperature synthesis of MFe_2O_4 (M=Co, Ni, Zn) superparamagnetic nano crystals. J Magn Magn Mater 2008;320:L70.
[10] Batoo Khalid Mujasam, Kumar Shalendra, Lee Chan Gyu, Alimuddin. Finite size effect and influence of temperature on electrical properties of nano crystalline Ni–Cd ferrites. Curr Appl Phys 2009;9:1072.
[11] Soibam I, phanjoubam S, Prakash C. Magnetic and Mössbauer studies of Ni substituted Li–Zn ferrite. J Magn Magn Mater 2009;321:2779.
[12] Raghasudha M, Ravinder D, Veerasomaiah P. Characterization of chromium substituted cobalt nano ferrites synthesized by citrate-gel auto combustion method. Adv Mater Phys Chem 2013;3:89–96.
[13] Venudhar YC, Satya Mohan K. Dielectric behavior of lithium–cobalt mixed ferrites. Mater. Lett 2002;54:135.
[14] Bellad SS, Chougule BK. Composition and frequency dependent dielectric properties of Li–Mg–Ti ferrites. Mater Chem Phys 2000;66:58.
[15] Ravinder D, Chandrashekhar Reddy A. Dielectric properties of Li–Ge ferrites. Mater Lett 2003;57:2855.
[16] Singh Amarendra K, Goel TC, Goel TG, Mendiratta RG, Thakur OP, Prakash Chandra. Dielectric properties of Mn-substituted Ni–Zn ferrite. J Appl Phys 2002;91:6626.

[17] Bhatu SS, Lakhani VK, Tanna AR. Effect of nickel substitution on structural, infrared and elastic properties of lithium ferrite. Indian J Pure Appl Phys 2007;45:596. IPC code GO1J3/28.
[18] Raghasudha M, Ravinder D, Veerasomaiah P. Characterization of nanostructured magnesium-chromium ferrites synthesized by citrate-gel auto combustion method. Adv Mat Lett 2013;4:910. http://dx.doi.org/10.5185/amlett.2013.5479.
[19] Raghasudha M, Ravinder D, Veerasomaiah P. FTIR studies and dielectric properties of Cr substituted cobalt nano ferrites synthesized by citrate-gel method. Nanosci Nanotech 2013;3:105. http://dx.doi.org/10.5923/j.nn.20130305.01.
[20] Pervaiz Erum, Gul IH. Enhancement of electrical properties due to C^{r3+} substitution in Co-ferrite nanoparticles synthesized by two chemical techniques. J Magn Magn Mater 2012;324:3695.
[21] Raghasudha M, Ravinder D, Veerasomaiah P. Thermoelectric power studies of Co–Cr nano ferrites. J Alloys Compd 2014;604:276.
[22] Morin FJ, Geballe TH. Electrical conductivity and seebeck effect in $Ni_{0.8}Fe_{2.2}O_4$. Phys Rev 1955;99:467.
[23] Priyadarshini P, Pradeep A, Sambasivarao P, Chandrasekaran G. Structural, spectroscopic and magnetic study of nanocrystalline Ni–Zn ferrites. Mater Chem Phys 2009;116:207.
[24] Tarte P. Infra-red spectrum and tetrahedral coordination of lithium in the spinel $LiCrGeO_4$. Acta Crystallogr 1963;16:228.
[25] Mazen SA, Abu-Elsaad NI. IR spectra, elastic and dielectric properties of Li–Mn ferrite. ISRN Condens Matter Phys 2012:9. http://dx.doi.org/10.5402/2012/907257. Article ID 907257.
[26] Kumar V, Rana A, Kumar N, Pant RP. Investigations on controlled size precipitated cobalt ferrite nano particles. Int J Appl Ceram Technol 2011;8:120.
[27] Samsonov D, Zhdanov S, Morfill G, Steinberg V. Levitation and agglomeration of magnetic grains in a complex (dusty) plasma with magnetic field. New J Phys 2003;5:24.1. http://dx.doi.org/10.1063/1.1763577.
[28] Rezlescu N, Rezlescu E. Dielectric properties of copper containing ferrites. Phys Status Solidi A 1974;23:575.
[29] Gul IH, Maqsood A, Naeem M, Naeem Ashiq M. Optical, magnetic and electrical investigation of cobalt ferrite nanoparticles synthesized by co-precipitation route. J Alloys Comp 2010;507:201.
[30] Iwauchi K. Dielectric properties of fine particles of Fe_3O_4 and some ferrites. Jap J Appl Phys 1971;10:1520.
[31] Maxwell JC. Electricity and magnetism, 1. Oxford: Oxford University Press; 1929 (section 328).
[32] Baruwati B, Reddy KM, Manorama SV, Singh RK, Prakash O. Tailored conductivity behavior in nanocrystalline nickel ferrite. App Phys Lett 2004;85:2833.
[33] Jonker GH. Analysis of the semiconducting properties of cobalt ferrite. J Phys Chem Solids 1959;9:165.
[34] Soibam I, Phanjoubam S, Sharma HB, Sarma HNK, Laishram R, Prakash C. Effects of cobalt substitution on the dielectric properties of Li–Zn ferrite. Solid State Comm 2008;148:399.
[35] Koops CG. On the dispersion of resistivity and dielectric constant of some semiconductors at audio frequencies. Phys Rev 1951;83:121.
[36] Sharifi Ibrahim, Shokrollahi H. Nanostructural, magnetic and Mössbauer studies of nanosized $Co_{1-x}Zn_xFe_2O_4$ synthesized by co-precipitation. J Magn Magn Mater 2012;324:2397.

Dr. M. Raghasudha is working as Associate Professor in Chemistry, Jayaprakash Narayan college of Engineering, Mahabubnagar, Telangana, India. She obtained her M.Sc. in Chemistry (1997) from Kakatiya University, Telangana, M.Phil. in Chemistry (2007) from Alagappa University, Tamil Nadu and Ph.D. from Osmania University, Hyderabad, Telangana, India in 2014. To her credit she has published 15 research papers in International Journals, attended 20 national and international conferences and has 19 years of teaching experience. Her current area of research is on electrical and magnetic properties of ferrite nano materials and thin films by citrate-gel method.

Prof. D. Ravinder is working as Professor and Head, Department of Physics, Nizam college, Osmania University, Hyderabad, Andhra Pradesh, India. His research work is on magnetic and electrical properties of ferrites, thin films, GMR materials, Cu-Co alloy thin films and nano-materials by pulsed laser deposition, sol gel, citrate precursor method and electro deposition. To his credit, he has published 195 research papers in International Journals. He has been awarded Young Scientist award received by Dr. Abdual Kalam (former president of India), for outstanding contributions in the field of science and Technology, UGC research award, Boyscast by DST (Department of science and technology), Government of India, JSPS fellowship Japan and Royal Society fellowship, UK. He also visited USA, UK, Sweden, Ireland, Singapore and Japan for Collaborative Research and invited talks.

Dr.G. Aravind is working as Asst. Professor in Physics, Methodist College of Engineering and Technology, Affiliated to Osmania University, Hyderabad. Telangana, India. He completed his M.Sc in 2007 and Ph.D. in 2015 from Osmania University, Hyderabad, Telangana, India. He published 5 international papers and attended 13 national and international conferences. He has four years teaching experience.